Single-Photon Cooling in Microwave Magnetomechanics

D. Zoepfl,[*,†] M. L. Juan,[*] C. M. F. Schneider, and G. Kirchmair[‡]
Institute for Quantum Optics and Quantum Information of the Austrian Academy of Sciences, A-6020 Innsbruck, Austria and Institute for Experimental Physics, University of Innsbruck, A-6020 Innsbruck, Austria

(Received 14 January 2020; revised 16 April 2020; accepted 1 June 2020; published 7 July 2020)

Cavity optomechanics, where photons are coupled to mechanical motion, provides the tools to control mechanical motion near the fundamental quantum limits. Reaching single-photon strong coupling would allow to prepare the mechanical resonator in non-Gaussian quantum states. Preparing massive mechanical resonators in such states is of particular interest for testing the boundaries of quantum mechanics. This goal remains however challenging due to the small optomechanical couplings usually achieved with massive devices. Here we demonstrate a novel approach where a mechanical resonator is magnetically coupled to a microwave cavity. We measure a single-photon coupling of $g_0/2\pi \sim 3$ kHz, an improvement of one order of magnitude over current microwave optomechanical systems. At this coupling we measure a large single-photon cooperativity with $C_0 \gtrsim 10$, an important step to reach single-photon strong coupling. Such a strong interaction allows us to cool the massive mechanical resonator to a third of its steady state phonon population with less than two photons in the microwave cavity. Beyond tests for quantum foundations, our approach is also well suited as a quantum sensor or a microwave to optical transducer.

DOI: 10.1103/PhysRevLett.125.023601

In recent years, cavity optomechanics has pushed the boundaries of quantum mechanics using micrometer-sized mechanical resonators. Among the accomplishments were ground state cooling of mechanical motion [1–3], measurement precision below the standard quantum limit [4,5], preparing mechanical resonators in nonclassical states [6–9] and entangling the mechanical state with the optical field [10–12]. In this context, an important parameter is the interaction strength between the mechanical and photonic modes: the optomechanical coupling. Recently, the ultrastrong coupling regime was reached where this coupling, enhanced by the photons in the cavity, exceeds both decay rates (cavity and mechanics) and is comparable to the mechanical frequency [13]. However, to achieve a nonlinear optomechanical interaction, the coupling has to be further increased in order to reach the single-photon strong coupling regime. This regime, where the single-photon coupling strength, g_0, exceeds both the linewidth of the cavity, κ, and the linewidth of the mechanical resonator, Γ_m, ($g_0 > \kappa, g_0 > \Gamma_m$) opens the door to prepare quantum superposition states in a mechanical resonator [14]. Large couplings can be achieved by using resonators with small masses [15,16] or by replacing the cavity by a qubit [17–21], although in the later case it is not possible to benefit from a photon enhanced coupling. Reaching the single-photon strong coupling regime with mechanical resonators having a large mass and long coherence time is of particular interest to investigate the classical to quantum transition [22]. This remains challenging since the coupling depends directly on the zero-point fluctuation of the resonator: massive resonators generally exhibit much smaller couplings [14].

A promising candidate for achieving single-photon strong coupling is microwave optomechanics, as it provides high quality cavities with much lower frequencies and is particularly well adapted to cryogenic operation [23]. To date, the favored approach for cavity optomechanics relies on a mechanically compliant element which modulates the capacitance of a microwave cavity. Ultimately bounded by the capacitor gap and the zero-point fluctuation amplitude of the resonator, state-of-the-art devices have reached couplings of a few hundreds of Hertz [14]. Achieving single-photon strong coupling presents extreme technological challenges in order to either increase the coupling strength g_0 or decrease the cavity linewidth substantially. An important step towards this regime is to achieve a large single-photon cooperativity [14], $C_0 = 4g_0^2/\kappa\Gamma_m$. For $C_0 > 1$, the backaction on the mechanical resonator from a single cavity photon is sufficient to enable cooling [24]. This regime was recently achieved in the optical regime with massive resonators [25], but remains challenging in the microwave regime due to the smaller coupling strengths.

Here we report on reaching a coupling strength in the kHz range, allowing us to demonstrate a single-photon cooperativity exceeding unity between a microwave cavity and a massive mechanical resonator. To increase the coupling, we propose an alternative to most microwave experiments by magnetically coupling the mechanical resonator to the cavity, an approach which gained attention recently [26–29]. Concretely, our mechanical resonator is a single clamped beam—a cantilever—with a magnetic tip. In order to mediate the optomechanical interaction, we

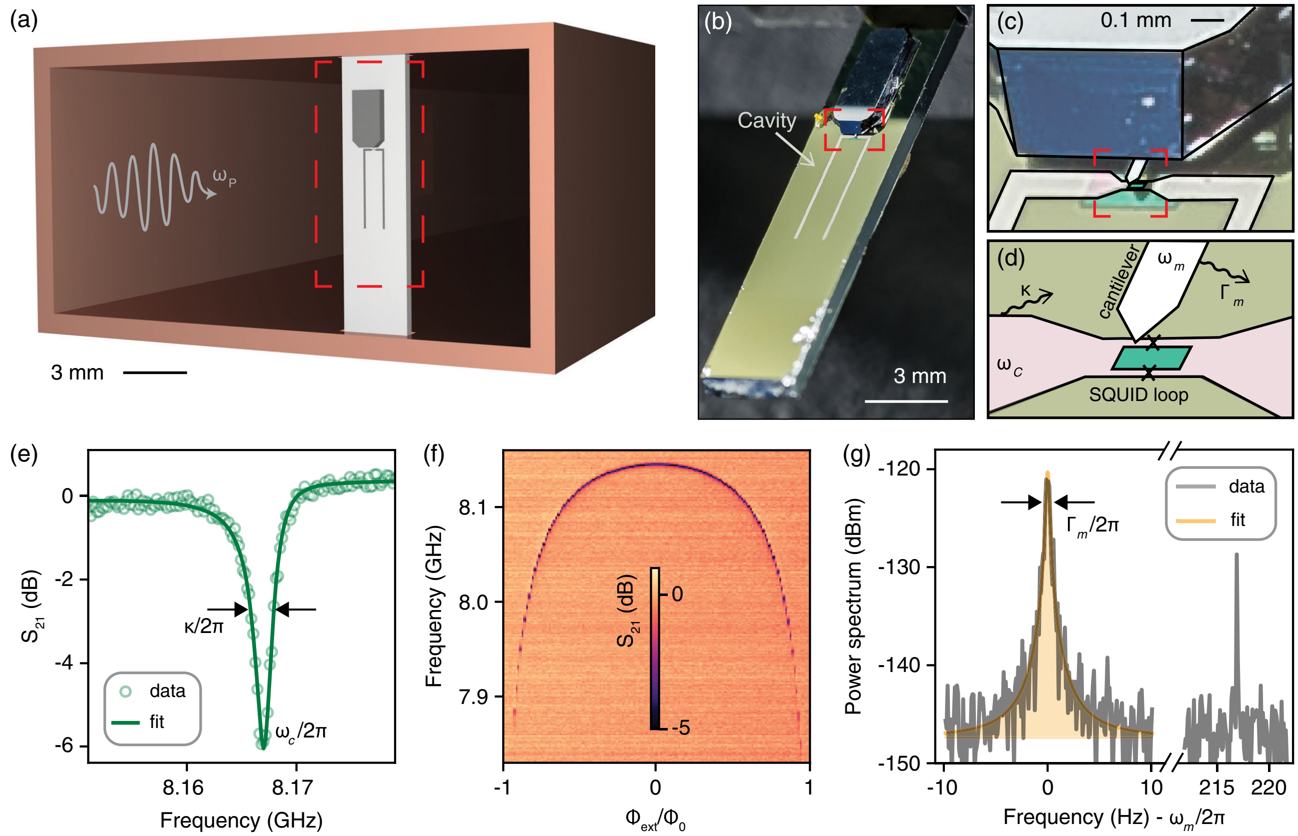

FIG. 1. General setup and device characterization. (a) Rectangular waveguide used to probe the microwave cavity, a U-shaped microstrip resonator on a silicon substrate. (b) Photograph of the device showing the microwave cavity and cantilever chip. (c) Closeup of the central part of the cavity including the SQUID and the mechanical resonator. (d) Sketch of the SQUID loop and cantilever. (e) Transmission measurement through the waveguide (notch configuration) showing the microwave cavity response. A fit to the data gives a frequency $\omega_c/2\pi = 8.167$ GHz and a linewidth $\kappa/2\pi = 2.8$ MHz. (f) Change of the microwave cavity frequency, obtained by transmission measurements, as a function of the applied external magnetic flux. (g) Thermal noise power spectrum of the cantilever at 100 mK after amplification and homodyne down mixing when probing the cavity with a weak resonant microwave tone of −54.5 dBm fridge input power. A fit to the power spectrum gives $\omega_m/2\pi = 274383.13 \pm 0.03$ Hz and $\Gamma_m/2\pi = 0.3 \pm 0.1$ Hz, the area below the curve (colored) corresponds to the motional energy of the cantilever mode. The sharp peak detuned ~215 Hz away from the mechanical frequency is the calibration peak [31].

integrated a superconducting quantum interference device (SQUID) in a U-shaped microstrip resonator [30] to effectively obtain a microwave cavity sensitive to magnetic flux. The single-photon coupling strength, g_0, is given by the change of the cavity frequency, ω_c, induced by the zero-point fluctuation, x_{ZPM}, of the mechanical resonator:

$$g_0 = \frac{\partial \omega_c}{\partial x} x_{\mathrm{ZPM}} = \frac{\partial \omega_c}{\partial \phi_{\mathrm{ext}}} \times \frac{\partial \phi_{\mathrm{ext}}}{\partial x} x_{\mathrm{ZPM}}. \tag{1}$$

As $\partial\omega_c/\partial x$ is not directly accessible it is more convenient to express the coupling in terms of external magnetic flux ϕ_{ext}. The second part, $\partial\phi_{\mathrm{ext}}/\partial x \times x_{\mathrm{ZPM}}$, gives the flux change induced by a zero-point motion of the mechanical cantilever. The first part describes the cavity frequency dependence on the flux through the SQUID loop hence providing a direct control of the coupling strength.

Our experiment is mounted to the base plate of a dilution refrigerator [31]. The microwave cavity is placed in a rectangular waveguide in order to provide a lossless microwave environment and control its coupling to the microwave probe tone traveling through the waveguide [see Fig. 1(a)]. We use the fundamental $\lambda/2$ mode with a current maximum at the centre, the position of the SQUID loop (see Fig. 1). For the mechanical resonator we use a commercial atomic force microscopy cantilever having a nominal room temperature frequency of 350 kHz and a mass of a few tens of nanograms [31]. To mediate the magnetic coupling to the cavity, we functionalized its tip with a strong micromagnet (NdFeB) and completed the sample by placing the cantilever 20 ± 1 μm above the SQUID, see Figs. 1(c) and 1(d).

The microwave cavity response is obtained via transmission measurements through the waveguide, Fig. 1(e) [31]. Fitting the model for a resonator in notch configuration [32,33] to our line shape gives a frequency $\omega_c/2\pi = 8.167$ GHz and a linewidth $\kappa/2\pi = 2.8$ MHz, where coupling to the waveguide and internal losses contribute equally to the linewidth with $\kappa_c/2\pi \simeq \kappa_I/2\pi \simeq$ 1.4 MHz. The internal losses set a lower bound on the total linewidth. To control the cavity frequency, an external magnetic field is applied through the SQUID loop by using coils, Fig. 1(f). The slope of the flux map gives the sensitivity to magnetic fields, $\partial\omega_c/\partial\phi_{\rm ext}$, which directly sets the coupling [Eq. (1)]. The mechanical resonator modulates the response of the microwave cavity at its frequency ω_m. We use a microwave probe tone close to the cavity resonance which, in the bad cavity limit $\kappa \gg \omega_m$, is amplitude modulated at the mechanical frequency. By performing a homodyne measurement we directly obtain the thermal noise power spectrum from the cantilever, Fig. 1(g). A fit with a damped harmonic resonator model gives a mechanical frequency $\omega_m/2\pi = 274383.13 \pm 0.03$ Hz and a linewidth $\Gamma_m/2\pi = 0.3 \pm 0.1$ Hz.

To extract the coupling between the cavity and the mechanical cantilever, we measure the thermal noise power spectrum, which depends on the bare coupling enhanced by the phonon number: $g_0\sqrt{n}$, but also on the transduction from the microwave cavity. To gain direct access to this transduction we apply a frequency modulation to the microwave probe tone [34,35]. Using such a calibration tone, Fig. 1(g), we get instant access to the transduction of the microwave cavity at the measurement point and directly obtain the value of $g_0\sqrt{n}$ from the power spectrum [31]. In addition, extracting the bare coupling g_0 requires knowledge of the phonon number. In the absence of optomechanical backaction and excessive vibrations, we expect the mechanical mode to be thermalized with the cyrostat, $\langle n^{\rm th}\rangle = 1/(e^{\hbar\omega_m/k_bT} - 1) \simeq k_BT/(\hbar\omega_m)$, where k_B is the Boltzmann constant, T the temperature and $\hbar$ the reduced Planck constant.

In order to verify that the mechanical mode is thermalized, we increased the temperature of our cryostat from 80 mK to 700 mK, Fig. 2(a), and measured $g_0\sqrt{n}$. Keeping g_0 constant, we expect an increase in $g_0\sqrt{n}$ due to an increasing phonon population with the cryostat temperature. By fitting the data assuming $\langle n\rangle = \langle n^{\rm th}\rangle$, we extract a bare coupling of $g_0/2\pi = 48 \pm 1$ Hz. To avoid any optomechanical backaction, we chose a point of weak coupling along with a moderate microwave probe tone of -54.5 dBm [31], as the photon enhanced coupling has to be considered for the backaction. This assumption is verified by ensuring $g_0\sqrt{n}$ is constant while varying the input power [31]. All the following measurements were done at 100 mK.

Next, we demonstrate the control of the coupling strength, $g_0 \propto \partial\omega_c/\partial\phi_{\rm ext}$, by changing the external flux bias. To avoid any backaction on the cantilever, we reduced the power in the microwave cavity according to the increasing flux sensitivity [31]. The measured coupling

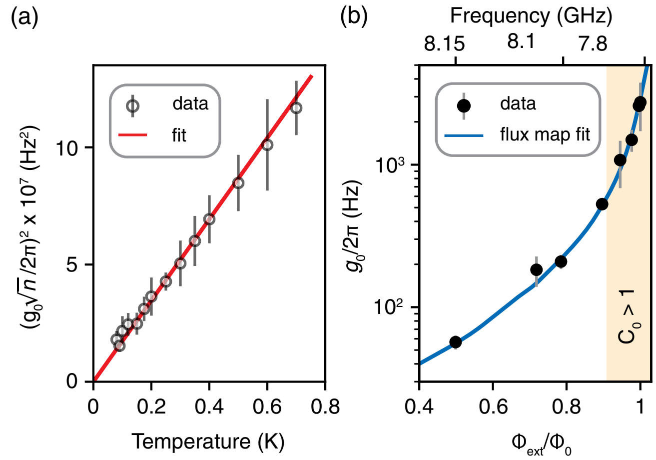

FIG. 2. Temperature ramp and coupling strength dependence with the flux bias point. (a) Measurement of $g_0\sqrt{n}$ with increasing cryostat temperature at a fixed sensitivity and fridge input power of -54.5 dBm [31]. We verify that the cantilever is thermalized with the cryostat temperature by fitting it assuming $\langle n\rangle = \langle n^{\rm th}\rangle$, obtaining a coupling $g_0/2\pi = 48 \pm 1$ Hz. (b) Measurement of the bare coupling strength for different flux bias points. The solid line is the sensitivity predicted from the slope of the flux map [Fig. 1(f)]. In the shaded region the coupling is sufficient to reach $C_0 > 1$. (a),(b), The error bar denotes the standard deviation of multiple measurements [31].

strength in dependence with the flux bias point is shown in Fig. 2(b). The solid line depicts the sensitivity, which is extracted from the derivative of the flux map, Fig. 1(f), where a fit to the data provides the flux change per phonon $\partial\phi_{\rm ext}/\partial x \times x_{\rm ZPM} = 1.60 \pm 0.05\ \mu\phi_0$. The main limitation for measuring higher couplings, in addition to increased flux instability during the 10 minutes measurement time, is the much lower signal as we reduced the incident probe power. For the highest couplings measured, $g_0/2\pi \sim 3$ kHz, we achieve a large single-photon cooperativity of $C_0 \gtrsim 10$.

While previous measurements were obtained with low enough input power to avoid backaction, we discuss in the following the possibility to cool the mechanical mode. By driving the cavity red detuned ($\omega_p < \omega_c$), inelastic anti-Stokes scattering is favored, which leads to cooling of the mechanical motion [14] [Fig. 3(a)]. In addition, such backaction is accompanied by a broadening of the mechanical linewidth and a frequency shift. Conversely, pumping blue detuned leads to heating of the mechanics and a decrease of the linewidth. Dynamical instability of the mechanical mode is reached when the linewidth approaches zero [36].

First, we demonstrate cavity cooling by operating at a low coupling, $g_0/2\pi = 57 \pm 7$ Hz [Fig. 2(b)]. For low power (open symbols in Fig. 3), we fit the back-action measurements using the theory for cavity-assisted cooling [31,36,37], obtaining an independent measurement of the maximum photon number of 186 ± 12 and the coupling

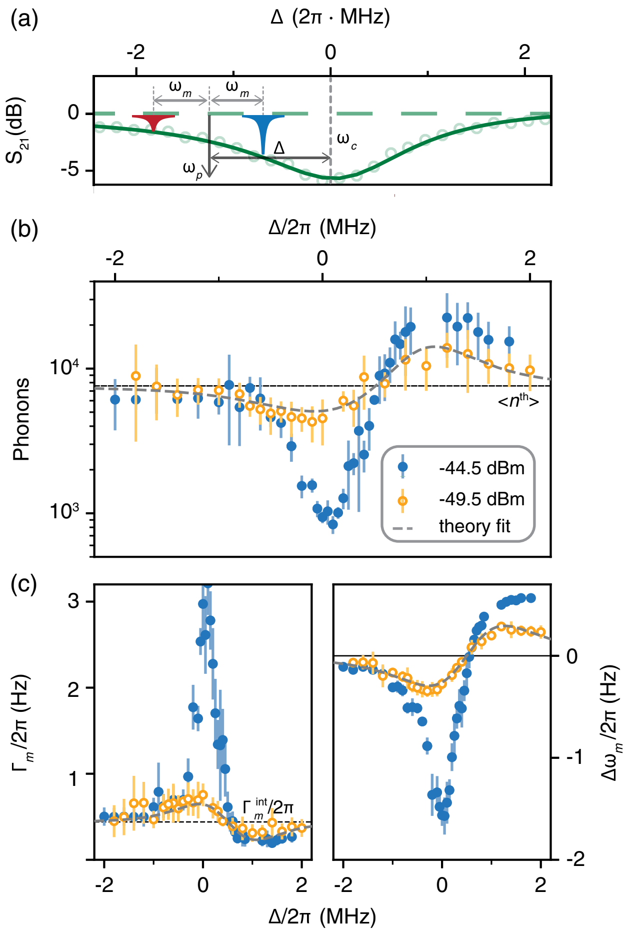

FIG. 3. Backaction measurements for small coupling, $g_0/2\pi = 57 \pm 7$ Hz. (a) Illustration of the cavity cooling mechanism for a pump tone ω_p, red detuned from the cavity, $\Delta = \omega_p - \omega_c < 0$. In blue and red are the anti-Stokes and Stokes scattering processes, respectively. (b) Phonon number in the mechanical cantilever against detuning of the pump for two different powers. The dashed line shows the thermal phonon number for the mode $\langle n^{\mathrm{th}} \rangle \simeq 7600$. (c) Change of linewidth and mechanical frequency against detuning of the pump. A fit of the phonon number with detuning for the lower power measurement gives a maximum photon number of 186 ± 12 and $g_0/2\pi = 57 \pm 1$ Hz. The predictions from the theoretical model using the extracted parameters are plotted in (b) and (c). (b),(c) The error bar denotes the propagated fit error of multiple measurements [31].

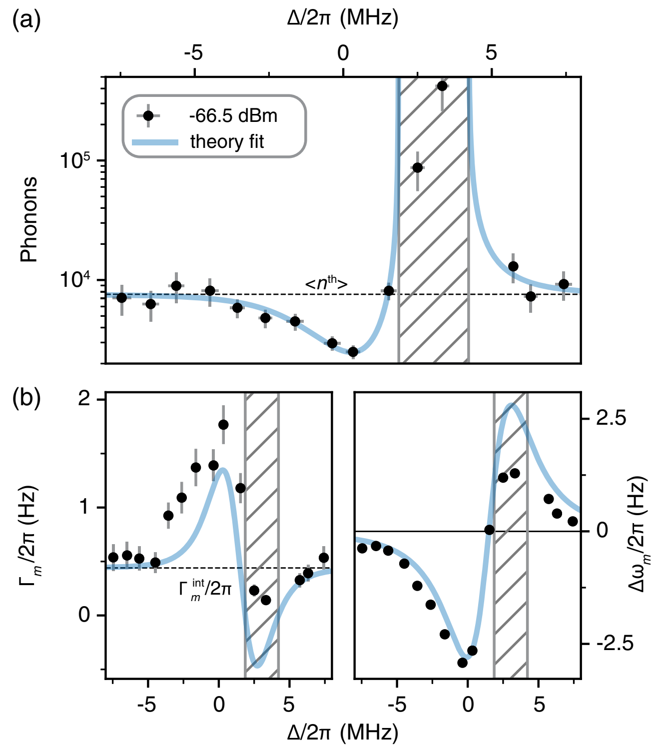

FIG. 4. Backaction measurements in the large coupling regime, where $C_0 \gtrsim 10$. (a) Phonon number against detuning. A fit provides the maximum photon number in the microwave cavity, 2.1 ± 0.4, and $g_0/2\pi = 2.38 \pm 0.06$ kHz. (b) Linewidth and frequency shift against detuning. We plot the theoretical predictions with the fit parameters obtained in panel (a). (a),(b) The hashed area marks the region of dynamical instability. The y-error bar denotes the propagated fit error of multiple measurements, the x error arises from our grouping method we apply to this data [31].

$g_0/2\pi = 57 \pm 1$ Hz. As expected, the change of phonon number is accompanied by a linewidth and frequency change [Fig. 3(c)]. We note that we also included a frequency offset to the fit to accommodate the impedance mismatch of the cavity with the waveguide [31]. For increasing input power the backaction increases, allowing us to achieve a nearly eightfold decrease from the thermal phonon occupation $\langle n^{\mathrm{th}} \rangle \simeq 7600$ to $\langle n \rangle = 970 \pm 130$, Fig. 3(b). Since we are in the bad cavity regime, the theoretical limit is given by $\langle n^{\mathrm{min}} \rangle = (\kappa/4\omega_m)^2 \simeq 6.5$ [36]. Practically, we were limited by the nonlinearity of the microwave cavity arising from the Josephson junctions. This effect prevents us from fitting the data for higher input power, but also sets an upper bound on the cavity photons of around 1200 before it becomes bistable [31,38]. The impact of the nonlinearity, while it constitutes an interesting element of study on its own [38], could be mitigated by further improving the cavity, for example by using a SQUID array.

To demonstrate cooling with a few photons, we work at a more flux sensitive point where we expect a coupling $g_0/2\pi = 2.3 \pm 0.3$ kHz [Fig. 2(b)] and a large cooperativity $C_0 \gtrsim 10$. By using an input power of -66.5 dBm, for which we expect an average occupation of around a single photon in the cavity, we clearly demonstrate cooling and heating of the cantilever mode, Fig. 4. By fitting the experimental data [31,36,37] we extract a maximum photon number of 2.1 ± 0.4, and a coupling of $g_0/2\pi = 2.38 \pm 0.06$ kHz. In terms of cooling, owing to the large cooperativity, we reached $\langle n \rangle = 2430 \pm 310$, corresponding to a cooling factor ~ 3 for a nanogram-scaled mechanical resonator. For the corresponding detuning, we extract a cavity population of only 1.4 photons [31]. We note that the mechanical linewidth is significantly larger than the theoretical prediction, an effect that we attribute to the high sensitivity to flux noise [31]. By increasing the incident power until the nonlinearity was too severe, we reached $\langle n\rangle \simeq 150$ with ~20 photons in average in the cavity.

To conclude, the novel approach for microwave optomechanics we demonstrate in this Letter relies on simple elements, namely a $\lambda/2$ superconducting resonator with an integrated SQUID for the cavity and a commercial cantilever for the mechanical resonator, providing an optomechanical g_0 in the kHz range. In the context of cavity optomechanics, this constitutes an improvement of one order of magnitude over couplings achieved in the microwave regime. Owing to this strong interaction, we achieved large single-photon cooperativities of $C_0 \gtrsim 10$ and demonstrated the cooling of the mechanical mode to a third of its thermal population with less than two photons in the cavity. Furthermore, owing to the 3D architecture of this approach, it offers numerous opportunities to significantly improve the optomechanical coupling as well as decreasing the microwave cavity linewidth, clearly paving the way to enter single-photon strong coupling. This would, most notably, facilitate preparing the massive mechanical resonator in non-Gaussian states, which can be used to perform fundamental tests on quantum mechanics. In addition, our approach can be used in more practical applications such as force sensing [41] and microwave-to-optics transduction [42].

We want to thank Hans Huebl for fruitful discussion. Further we thank our in-house mechanical workshop. D. Z. and M. L. J. are funded by the European Union' s Horizon 2020 research and innovation program under Grant Agreement No. 736943. C. M. F. S. is supported by the Austrian Science Fund FWF within the DK-ALM (W1259-N27).

[*]These authors contributed equally to this work.
[†]david.zoepfl@uibk.ac.at
[‡]gerhard.kirchmair@uibk.ac.at

[1] A. D. O'Connell, M. Hofheinz, M. Ansmann, R. C. Bialczak, M. Lenander, E. Lucero, M. Neeley, D. Sank, H. Wang, M. Weides, J. Wenner, J. M. Martinis, and A. N. Cleland, Quantum ground state and single-phonon control of a mechanical resonator, Nature (London) **464**, 697 (2010).

[2] J. D. Teufel, T. Donner, D. Li, J. W. Harlow, M. S. Allman, K. Cicak, A. J. Sirois, J. D. Whittaker, K. W. Lehnert, and R. W. Simmonds, Sideband cooling of micromechanical motion to the quantum ground state, Nature (London) **475**, 359 (2011).

[3] J. Chan, T. P. M. Alegre, A. H. Safavi-Naeini, J. T. Hill, A. Krause, S. Gröblacher, M. Aspelmeyer, and O. Painter, Laser cooling of a nanomechanical oscillator into its quantum ground state, Nature (London) **478**, 89 (2011).

[4] J. D. Teufel, T. Donner, M. A. Castellanos-Beltran, J. W. Harlow, and K. W. Lehnert, Nanomechanical motion measured with an imprecision below that at the standard quantum limit, Nat. Nanotechnol. **4**, 820 (2009).

[5] G. Anetsberger, E. Gavartin, O. Arcizet, Q. P. Unterreithmeier, E. M. Weig, M. L. Gorodetsky, J. P. Kotthaus, and T. J. Kippenberg, Measuring nanomechanical motion with an imprecision below the standard quantum limit, Phys. Rev. A **82**, 061804 (2010).

[6] E. E. Wollman, C. U. Lei, A. J. Weinstein, J. Suh, A. Kronwald, F. Marquardt, A. A. Clerk, and K. C. Schwab, Quantum squeezing of motion in a mechanical resonator, Science **349**, 952 (2015).

[7] F. Lecocq, J. B. Clark, R. W. Simmonds, J. Aumentado, and J. D. Teufel, Quantum Nondemolition Measurement of a Nonclassical State of a Massive Object, Phys. Rev. X **5**, 041037 (2015).

[8] J.-M. Pirkkalainen, E. Damskägg, M. Brandt, F. Massel, and M. A. Sillanpää, Squeezing of Quantum Noise of Motion in a Micromechanical Resonator, Phys. Rev. Lett. **115**, 243601 (2015).

[9] A. P. Reed, K. H. Mayer, J. D. Teufel, L. D. Burkhart, W. Pfaff, M. Reagor, L. Sletten, X. Ma, R. J. Schoelkopf, E. Knill, and K. W. Lehnert, Faithful conversion of propagating quantum information to mechanical motion, Nat. Phys. **13**, 1163 (2017).

[10] T. A. Palomaki, J. D. Teufel, R. W. Simmonds, and K. W. Lehnert, Entangling mechanical motion with microwave fields, Science **342**, 710 (2013).

[11] R. Riedinger, A. Wallucks, I. Marinković, C. Löschnauer, M. Aspelmeyer, S. Hong, and S. Gröblacher, Remote quantum entanglement between two micromechanical oscillators, Nature (London) **556**, 473 (2018).

[12] C. F. Ockeloen-Korppi, E. Damskägg, J.-M. Pirkkalainen, M. Asjad, A. A. Clerk, F. Massel, M. J. Woolley, and M. A. Sillanpää, Stabilized entanglement of massive mechanical oscillators, Nature (London) **556**, 478 (2018).

[13] G. A. Peterson, S. Kotler, F. Lecocq, K. Cicak, X. Y. Jin, R. W. Simmonds, J. Aumentado, and J. D. Teufel, Ultrastrong Parametric Coupling between a Superconducting Cavity and a Mechanical Resonator, Phys. Rev. Lett. **123**, 247701 (2019).

[14] M. Aspelmeyer, T. J. Kippenberg, and F. Marquardt, Cavity optomechanics, Rev. Mod. Phys. **86**, 1391 (2014).

[15] F. Brennecke, S. Ritter, T. Donner, and T. Esslinger, Cavity Optomechanics with a Bose-Einstein Condensate, Science **322**, 235 (2008).

[16] K. W. Murch, K. L. Moore, S. Gupta, and D. M. Stamper-Kurn, Observation of quantum-measurement backaction with an ultracold atomic gas, Nat. Phys. **4**, 561 (2008).

[17] J.-M. Pirkkalainen, S. U. Cho, F. Massel, J. Tuorila, T. T. Heikkilä, P. J. Hakonen, and M. A. Sillanpää, Cavity optomechanics mediated by a quantum two-level system, Nat. Commun. **6**, 6981 (2015).

[18] Y. Chu, P. Kharel, T. Yoon, L. Frunzio, P. T. Rakich, and R. J. Schoelkopf, Creation and control of multi-phonon Fock states in a bulk acoustic-wave resonator, Nature (London) **563**, 666 (2018).

[19] J. J. Viennot, X. Ma, and K. W. Lehnert, Phonon-Number-Sensitive Electromechanics, Phys. Rev. Lett. **121**, 183601 (2018).

[20] P. Delsing *et al.*, The 2019 surface acoustic waves roadmap, J. Phys. D **52**, 353001 (2019).

[21] T. Bera, S. Majumder, S. K. Sahu, and V. Singh, Large flux-mediated coupling in hybrid electromechanical system with a transmon qubit, arXiv:2001.05700.

[22] M. Arndt and K. Hornberger, Testing the limits of quantum mechanical superpositions, Nat. Phys. **10**, 271 (2014).

[23] C. A. Regal and K. W. Lehnert, From cavity electromechanics to cavity optomechanics, J. Phys. Conf. Ser. **264**, 012025 (2011).

[24] M. Yuan, V. Singh, Y. M. Blanter, and G. A. Steele, Large cooperativity and microkelvin cooling with a three-dimensional optomechanical cavity, Nat. Commun. **6**, 8491 (2015).

[25] J. Guo, R. Norte, and S. Gröblacher, Feedback Cooling of a Room Temperature Mechanical Oscillator close to its Motional Ground State, Phys. Rev. Lett. **123**, 223602 (2019).

[26] G. Via, G. Kirchmair, and O. Romero-Isart, Strong Single-Photon Coupling in Superconducting Quantum Magnetomechanics, Phys. Rev. Lett. **114**, 143602 (2015).

[27] I. C. Rodrigues, D. Bothner, and G. A. Steele, Coupling microwave photons to a mechanical resonator using quantum interference, Nat. Commun. **10**, 5359 (2019).

[28] X. Wang, H. R. Li, P. B. Li, C. W. Jiang, H. Gao, and F. L. Li, Preparing ground states and squeezed states of nanomechanical cantilevers by fast dissipation, Phys. Rev. A **90**, 013838 (2014).

[29] P. Schmidt, M. T. Amawi, S. Pogorzalek, F. Deppe, A. Marx, R. Gross, and H. Huebl, Sideband-resolved resonator electromechanics on the single-photon level based on a nonlinear Josephson inductance, arXiv:1912.08731.

[30] D. Zoepfl, P. R. Muppalla, C. M. F. Schneider, S. Kasemann, S. Partel, and G. Kirchmair, Characterization of low loss microstrip resonators as a building block for circuit QED in a 3d waveguide, AIP Adv. **7**, 085118 (2017).

[31] See the Supplemental Material at http://link.aps.org/supplemental/10.1103/PhysRevLett.125.023601, which includes Refs. [14], [30,32–40], for additional information on the sample preparation, the measurement setup and characterization measurements, the measurement protocol and data treatment, data on the temperature dependence of the device parameters, dependence of the cooperativity on the cavity bias point, and estimations of the maximum photon number.

[32] S. Probst, F. B. Song, P. A. Bushev, A. V. Ustinov, and M. Weides, Efficient and robust analysis of complex scattering data under noise in microwave resonators, Rev. Sci. Instrum. **86**, 024706 (2015).

[33] M. S. Khalil, M. J. A. Stoutimore, F. C. Wellstood, and K. D. Osborn, An analysis method for asymmetric resonator transmission applied to superconducting devices, J. Appl. Phys. **111**, 054510 (2012).

[34] M. L. Gorodetksy, A. Schliesser, G. Anetsberger, S. Deleglise, and T. J. Kippenberg, Determination of the vacuum optomechanical coupling rate using frequency noise calibration, Opt. Express **18**, 23236 (2010).

[35] X. Zhou, F. Hocke, A. Schliesser, A. Marx, H. Huebl, R. Gross, and T. J. Kippenberg, Slowing, advancing and switching of microwave signals using circuit nanoelectromechanics, Nat. Phys. **9**, 179 (2013).

[36] F. Marquardt, J. P. Chen, A. A. Clerk, and S. M. Girvin, Quantum Theory of Cavity-Assisted Sideband Cooling of Mechanical Motion, Phys. Rev. Lett. **99**, 093902 (2007).

[37] A. H. Safavi-Naeini, J. Chan, J. T. Hill, S. Gröblacher, H. Miao, Y. Chen, M. Aspelmeyer, and O. Painter, Laser noise in cavity-optomechanical cooling and thermometry, New J. Phys. **15**, 035007 (2013).

[38] P. D. Nation, M. P. Blencowe, and E. Buks, Quantum analysis of a nonlinear microwave cavity-embedded dc SQUID displacement detector, Phys. Rev. B **78**, 104516 (2008).

[39] M. Yuan, M. A. Cohen, and G. A. Steele, Silicon nitride membrane resonators at millikelvin temperatures with quality factors exceeding 10^8, Appl. Phys. Lett. **107**, 263501 (2015).

[40] G. P. Agrawal and H. J. Carmichael, Optical bistability through nonlinear dispersion and absorption, Phys. Rev. A **19**, 2074 (1979).

[41] H. J. Mamin and D. Rugar, Sub-attonewton force detection at millikelvin temperatures, Appl. Phys. Lett. **79**, 3358 (2001).

[42] R. W. Andrews, R. W. Peterson, T. P. Purdy, K. Cicak, R. W. Simmonds, C. A. Regal, and K. W. Lehnert, Bidirectional and efficient conversion between microwave and optical light, Nat. Phys. **10**, 321 (2014).